



## OPEN ACCESS

## EDITED BY

Xiaoyi Duan,  
The First Affiliated Hospital of Xi'an  
Jiaotong University, China

## REVIEWED BY

Sara Colantonio,  
Institute of Information Science and  
Technologies of the National Research  
Council of Italy, Italy  
Radka Stoyanova,  
University of Miami, United States

## \*CORRESPONDENCE

Anant Madabhushi

✉ anantm@emory.edu

Rakesh Shiradkar

✉ rshirad@emory.edu

RECEIVED 14 February 2023

ACCEPTED 24 July 2023

PUBLISHED 05 September 2023

## CITATION

Midya A, Hiremath A, Huber J, Sankar  
Viswanathan V, Omil-Lima D, Mahran A,  
Bittencourt LK, Harsha Tirumani S,  
Ponsky L, Shiradkar R and Madabhushi A  
(2023) Delta radiomic patterns on serial  
bi-parametric MRI are associated with  
pathologic upgrading in prostate  
cancer patients on active surveillance:  
preliminary findings.  
*Front. Oncol.* 13:1166047.  
doi: 10.3389/fonc.2023.1166047

## COPYRIGHT

© 2023 Midya, Hiremath, Huber,  
Sankar Viswanathan, Omil-Lima, Mahran,  
Bittencourt, Harsha Tirumani, Ponsky,  
Shiradkar and Madabhushi. This is an open-  
access article distributed under the terms of  
the [Creative Commons Attribution License  
\(CC BY\)](https://creativecommons.org/licenses/by/4.0/). The use, distribution or  
reproduction in other forums is permitted,  
provided the original author(s) and the  
copyright owner(s) are credited and that  
the original publication in this journal is  
cited, in accordance with accepted  
academic practice. No use, distribution or  
reproduction is permitted which does not  
comply with these terms.

# Delta radiomic patterns on serial bi-parametric MRI are associated with pathologic upgrading in prostate cancer patients on active surveillance: preliminary findings

Abhishek Midya<sup>1</sup>, Amogh Hiremath<sup>2</sup>, Jacob Huber<sup>3</sup>,  
Vidya Sankar Viswanathan<sup>1</sup>, Danly Omil-Lima<sup>4</sup>, Amr Mahran<sup>5</sup>,  
Leonardo K. Bittencourt<sup>6</sup>, Sree Harsha Tirumani<sup>6</sup>, Lee Ponsky<sup>7</sup>,  
Rakesh Shiradkar<sup>1\*</sup> and Anant Madabhushi<sup>1,8\*</sup>

<sup>1</sup>Department of Biomedical Engineering, Emory University, Atlanta, GA, United States, <sup>2</sup>Picture Health, Cleveland, OH, United States, <sup>3</sup>Department of Biomedical Engineering, Case Western Reserve University, Cleveland, OH, United States, <sup>4</sup>Fox Chase Cancer Center, Philadelphia, PA, United States, <sup>5</sup>Department of Urology, Assiut University, Assiut, Egypt, <sup>6</sup>Department of Radiology, University Hospitals, Cleveland Medical Center, Cleveland, OH, United States, <sup>7</sup>Department of Urology, University Hospitals, Cleveland Medical Center, Cleveland, OH, United States, <sup>8</sup>Atlanta Veterans Administration Medical Center, Atlanta, GA, United States

**Objective:** The aim of this study was to quantify radiomic changes in prostate cancer (PCa) progression on serial MRI among patients on active surveillance (AS) and evaluate their association with pathologic progression on biopsy.

**Methods:** This retrospective study comprised  $N = 121$  biopsy-proven PCa patients on AS at a single institution, of whom  $N = 50$  at baseline conformed to the inclusion criteria. ISUP Gleason Grade Groups (GGG) were obtained from 12-core TRUS-guided systematic biopsies at baseline and follow-up. A biopsy upgrade (AS+) was defined as an increase in GGG (or in number of positive cores) and no upgrade (AS-) was defined when GGG remained the same during a median period of 18 months. Of  $N = 50$  patients at baseline,  $N = 30$  had MRI scans available at follow-up (median interval = 18 months) and were included for delta radiomic analysis. A total of 252 radiomic features were extracted from the PCa region of interest identified by board-certified radiologists on 3T bi-parametric MRI [T2-weighted (T2W) and apparent diffusion coefficient (ADC)]. Delta radiomic features were computed as the difference of radiomic feature between baseline and follow-up scans. The association of AS+ with age, prostate-specific antigen (PSA), Prostate Imaging Reporting and Data System (PIRADS v2.1) score, and tumor size was evaluated at baseline and follow-up. Various prediction models were built using random forest (RF) classifier within a threefold cross-validation framework leveraging baseline radiomics ( $C_{br}$ ), baseline radiomics + baseline clinical ( $C_{brbcl}$ ), delta radiomics ( $C_{\Delta r}$ ), delta radiomics + baseline clinical ( $C_{\Delta r bcl}$ ), and delta radiomics + delta clinical ( $C_{\Delta r \Delta cl}$ ).

**Results:** An AUC of  $0.64 \pm 0.09$  was obtained for  $C_{br}$ , which increased to  $0.70 \pm 0.18$  with the integration of clinical variables ( $C_{brbcl}$ ).  $C_{\Delta r}$  yielded an AUC of  $0.74 \pm 0.15$ . Integrating delta radiomics with baseline clinical variables yielded an AUC of  $0.77 \pm 0.23$ .  $C_{\Delta r, \Delta cl}$  resulted in the best AUC of  $0.84 \pm 0.20$  ( $p < 0.05$ ) among all combinations.

**Conclusion:** Our preliminary findings suggest that delta radiomics were more strongly associated with upgrade events compared to PIRADS and other clinical variables. Delta radiomics on serial MRI in combination with changes in clinical variables (PSA and tumor volume) between baseline and follow-up showed the strongest association with biopsy upgrade in PCa patients on AS. Further independent multi-site validation of these preliminary findings is warranted.

#### KEYWORDS

active surveillance, prostate cancer, radiomics, magnetic resonance imaging, pathologic upgrade

## 1 Introduction

Prostate cancer (PCa) is the second leading cause of cancer-related mortality among men in the United States with nearly 34,500 expected deaths in 2022 (1). However, patients with low or favorable risk PCa do not need radical therapies and can safely be monitored via active surveillance (AS) as demonstrated in the PRIAS study (2), which showed excellent 10-year outcomes in men on AS (2). Patients on AS are usually followed up with serum prostate-specific antigen (PSA) every 6 months, a digital rectal exam (DRE) once a year, and repeat prostate biopsies (PBx) with or without MRI every 12 months or as needed, as per the National Comprehensive Cancer Network (NCCN) guidelines (3–5). The recent guidelines (5) have reestablished AS to be the preferred management strategy for low-risk PCa patients to curb overdiagnosis and overtreatment in men with PCa.

Current standard of care for men on AS is heavily reliant on monitoring via repeat fusion biopsies, which are invasive and expensive; cause discomfort to patients; carry the risk of bleeding, infection, and urinary retention; and are subject to sampling error (6). While MRI-targeted biopsies (7) have been shown to improve PCa localization, there is considerable debate as to whether patients could safely be monitored non-invasively via MRI without the need for invasive biopsies. Anxiety of untreated cancer arising out of this uncertainty (8, 9) is one of the important factors responsible for men discontinuing AS and opt for definitive treatment (2, 10). Besides invasive biopsies, DRE is routinely performed as part of AS (11), which is a source of discomfort and anxiety to patients and associated with false-positive readings (12). Consequently, an accurate, non-invasive imaging-based strategy for identifying candidates for AS and their monitoring is highly desirable.

Studies (13, 14) have shown MRI to be promising in identifying PCa patients suitable for AS; however, this is limited to initial risk stratification. Monitoring of PCa patients on AS using serial MRI showed a high negative predictive value but a moderate positive

predictive value and currently cannot replace biopsies. Radiologist assigned Prostate Imaging Reporting and Data System (PIRADS v2.1) scores have been studied (15) for patient triage to minimize repeat biopsies and improve quality of life; however, no objective guidelines exist for non-invasive monitoring. The Prostate Cancer Radiological Estimation of Change in Sequential Evaluation (PRECISE) (16) criteria have been proposed to monitor PCa progression on MRI using standardized guidelines. While upgrading in MRI-negative men was substantially lower compared to MRI-positive men, PRECISE criteria alone were insufficient to monitor and predict upgrading in MRI-positive men (13). Confirmatory systematic and targeted biopsies are still required to monitor patients on AS, despite the use of serial MRI. Clinical factors including PSA density have been studied and demonstrated to identify candidates for AS (17). PSA density in conjunction with MRI has been explored as a dynamic risk prediction strategy to monitor patients on AS (18). However, conclusive and objective guidelines for risk estimation of disease progression on AS are limited. Therefore, there is currently a critical need to improve MRI-based interpretation of PCa progression in conjunction with routine clinical factors including PSA to achieve non-invasive monitoring for AS.

Radiomics from prostate MRI have shown significant promise in characterization and risk stratification of PCa (19). Radiomics involves high-throughput extraction of quantitative measurements of subtle image texture and heterogeneity patterns using advanced image processing techniques that are not apparent on routine visual inspection. Bi-parametric MRI (bpMRI) that includes T2W and DWI sequences was shown (20, 21) to be efficient and non-inferior in diagnostic performance in comparison to multiparametric MRI (which includes contrast enhanced MRI). We hypothesize that “delta” changes in the progression of PCa on AS can be quantified using radiomic features on serial bpMRI. In this preliminary proof-of-concept study, we explore radiomic features from PCa regions on serial bpMRI (baseline and follow-up) along

with routine clinical parameters for their association with PCa progression on AS. We employ a single institutional dataset consisting of  $N = 50$  PCa patients on AS who underwent baseline followed by repeat 3T MRI on  $N = 30$  patients along with confirmatory systematic biopsies. We compare our integrated approach combining radiomics with clinical variables against radiologist assigned PIRADS v2.1 scores in predicting biopsy upgrade for PCa AS.

## 2 Methods

### 2.1 Patient selection

This HIPAA-compliant, retrospective study was approved by the local institutional review board (IRB) that waived the need for informed consent. A chart review was performed to include patients diagnosed with biopsy-proven PCa between 2012 and 2020 according to the following criteria: (a) patients with histopathologically documented PCa who were enrolled on AS, (b) availability of 3T MRI and systematic biopsy at baseline, (c)

followed up with PSA measurements and biopsies at least every 12 months for  $\geq 3$  years, and (d) including at least one additional 3T MRI between 18 and 36 months (see Figure 1). Patients with (a) imaging artifacts, (b) non-visible lesions, (c) negative biopsy at baseline, (d) non-availability of at least T2W and DWI sequences at baseline and follow-up, (e) discordant imaging and pathology findings, (f) different location of positive biopsy core at baseline and follow-up, and (g) disappeared lesion/newly detected location at follow-up were excluded from the study. All images were acquired with 3T MRI scanners (Siemens Skyra and Philips Ingenia) using pelvic phased array surface coil. The acronyms used in this manuscript are provided in Table 1. Detailed imaging parameters and characteristics are provided in Table 2. The International Society of Urological Pathology (ISUP) Gleason Grade Groups (GGG) were determined from 12-core transrectal ultrasound (TRUS)-guided systematic biopsies at baseline and follow-up. A biopsy upgrade (AS+) was defined as an increase in GGG from baseline 1 to  $\geq 2$  (increase in number of positive cores for baseline GGG = 2) at follow-up and no upgrade (AS-) when GGG remained the same. Detailed information about the patient cohort is provided in Table 3.

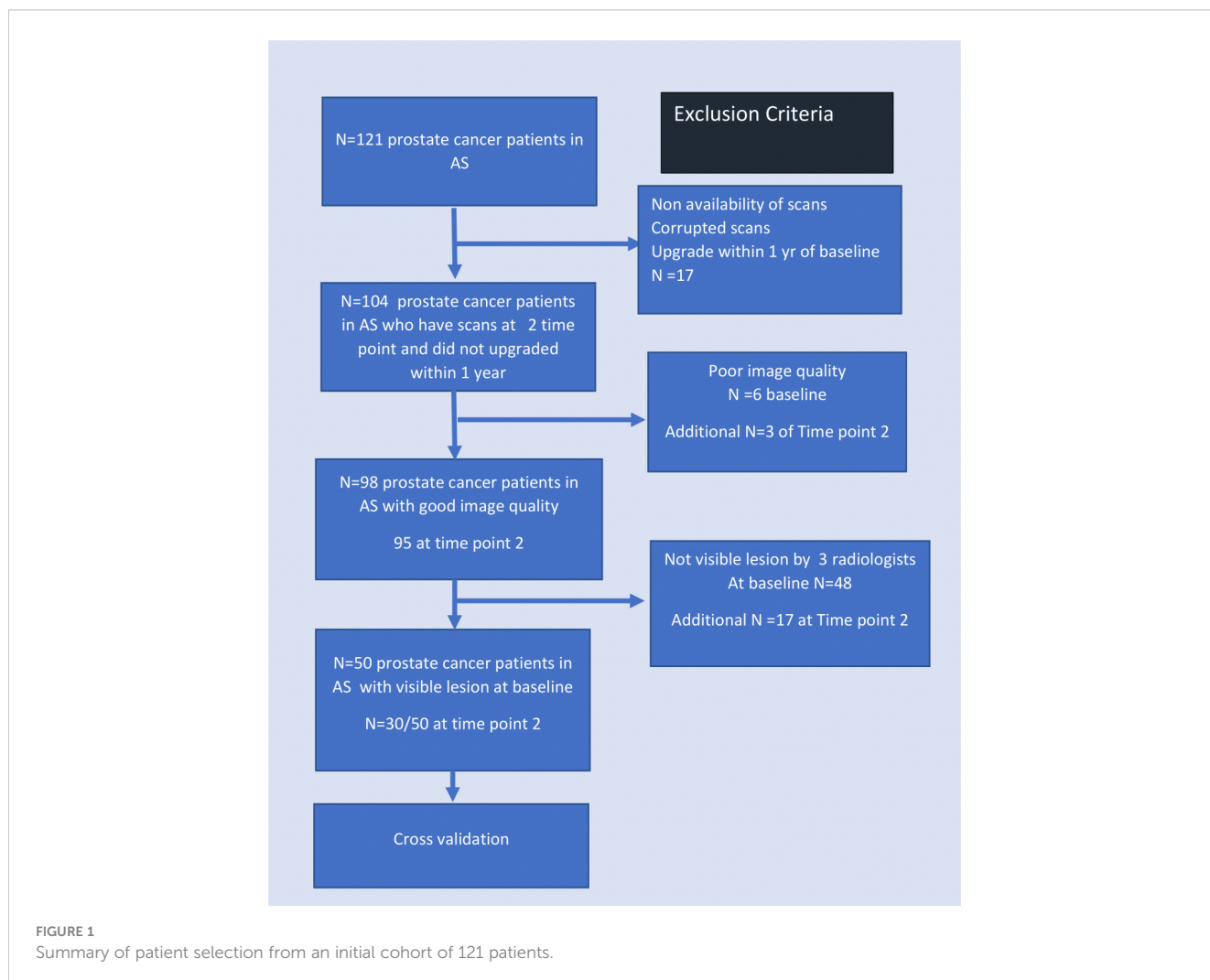


TABLE 1 List of acronyms used throughout the manuscript.

Name	Abbreviation
Baseline Radiomic Features	$F_r$
Baseline Clinical Features	$F_{cl}$
Delta Radiomic Features	$F_{\Delta r}$
Baseline Imaging Model	$C_{br}$
Baseline Clinical Model	$C_{bcl, x \in \{PSA, Tumor Volume\}}$
Baseline Integrated Model	$C_{brbcl}$
Delta Radiomic Model	$C_{\Delta r}$
Integrated Delta Radiomic and Baseline Model	$C_{\Delta r bcl}$
Delta Integrated Model	$C_{\Delta r \Delta cl}$
Prostate Imaging Reporting & Data System	PIRADS
Prostate Biopsy	PBx
Prostate Cancer	PCa
Clinically Significant Prostate Cancer	csPCa
Active Surveillance	AS

## 2.2 Prostate cancer delineations on MRI

Two board-certified genitourinary radiologists with greater than 10 years of experience in prostate imaging reviewed all the MRIs and delineated PCa regions of interest (ROI) on T2W and ADC. The readers were provided with the baseline and follow-up scans separately and were blinded to the relationship between the two sets of scans. They were also blinded to pathology results as well as positive core locations to avoid radiologists' bias in identifying PCa lesions. The readers were provided with high-resolution T2W, high  $b$ -value DWI and ADC images in the axial plane along with DCE sequences when available. ROI delineations were made by the reader on the T2W slice using the MD.AI software (22). The readers

TABLE 2 MRI parameters.

Parameters	Scanner
Manufacturer	(Siemens Healthcare, Erlangen, Germany), (Philips Medical Systems, Best, Netherlands)
Model	(3T Skyra), 3T Ingenia
<i>T2-weighted MR imaging</i>	
Repetition time/echo time (TR/TE)	3,894–8,740/90–150
Reconstruction spatial resolution (mm <sup>3</sup> )	0.56–1.25 × 0.56–1.25 × 2–3.5
<i>Diffusion-weighted imaging</i>	
Repetition time/echo time (TR/TE)	3,656–11,300/64–83
Reconstruction spatial resolution (mm <sup>3</sup> )	0.87–1.5 × 0.87–1.5 × 3–3.5
$b$ -values (s/mm <sup>2</sup> )	0, 500, 1,000, 1,500, 2,000–0, 400, 900, 1,500

could choose to delineate a lesion if visible or label the scan as negative on MRI or of poor diagnostic quality. The readers assigned PIRADS v2.1 scores to all lesions. A subset of patients was assigned to both radiologists to evaluate inter-reader variations in PCa delineation as well as PIRADS v2.1 scoring.

ROIs delineated by readers were later matched against positive biopsy core location obtained from systematic biopsies. Patients whose MRI scans were not assigned a PIRADS v2.1 score due to poor image quality or those that did not match with positive biopsy core locations were excluded from the study. In patients with multiple lesions, the lesion corresponding to the highest PIRADS v2.1 score and corresponding positive biopsy core location was included. The above-described rigorous steps were followed to ensure that no reader bias was introduced while identifying PCa ROIs on MRI.

## 2.3 Preprocessing of MRI

Prostate cancer ROIs were delineated by the radiologists on T2W as they provide the greatest anatomic resolution. ADC was co-registered to T2W using a rigid transformation using the Elastix toolbox (23, 24) (specific parameters are provided in the Supplementary Material), which was used to map PCa ROIs onto ADC. These ROIs were verified by radiologists and modified if they were not correctly aligned with the corresponding suspicious region on ADC. When there was significant deformation in ADC that could not be accounted through rigid transformation, separate ROIs were delineated for ADC.

Intra-patient intensity drift artifacts may cause image intensities to lack in tissue-specific meaning. This was corrected using a previously presented MRI intensity standardization method (25), which normalizes the histogram of intensities from a given region against a template image delivering tissue-specific intensity range. A pre-identified template using a subset of scan was used as a reference against which all scans in this study were mapped. This ensures that T2W measurements were normalized and reflect a tissue-specific meaning. Although we standardize the T2 scans, we did not standardize ADC scans since they are from single site and quantitative map.

## 2.4 Radiomic feature extraction

From the radiologist-delineated PCa ROIs on T2W and ADC, a set of 252 radiomic features were extracted using in-house software. These include first- and second-order statistics (mean, median, standard deviation, and range); 13 Haralick features (26), which are statistics derived from gray-level co-occurrence matrix (entropy, energy, inertia, inverse difference moment, marginal distributions, correlation, information measures of correlation, sum of average, sum of variance, sum of entropy, difference of average, difference of variance, difference of entropy, and contrast) computed at a window size of 3 × 3, 5 × 5, and 7 × 7; 5 Gabor features; and 1 CoLIAGe (27) feature. Radiomic features were extracted and processed in agreement with the image biomarker standardization initiative

TABLE 3 Patient demographics.

Clinical Predictor	AS+ (n = 28)	AS- (n = 22)	p-value
	Median value [range]		
Age (years)	68 [52–80]	66 [52–77]	
PSA at diagnosis (mg/ml)	5.91 [2.36–16.98]	4.61 [13.61–1.11]	<0.0005
PIRADS at diagnosis	[3–4]	[3–5]	<0.0005
PSA at follow-up	8.165 [2.35–18.93]	6.46 [4–11.2]	
PIRADS at follow-up	[3–5]	[3–5]	
Time interval between diagnosis and upgradation (months)	17.5 [8–45]	15.5 [4–57]	

(IBSI) criteria (28). Features were extracted on each 2D slice of T2W and ADC volumes with a delineated PCa ROI. Distribution statistics (mean, variance, skewness, and kurtosis) of each of these features over the entire lesion were computed to obtain a single feature vector per lesion.

Radiomic features were extracted from the baseline as well as follow-up bpMRI. Delta radiomics ( $F_{\Delta r}$ ) were computed as the difference in feature vector between baseline ( $F_{br}$ ) and follow-up, which quantify radiomic changes in lesion heterogeneity. Additional details regarding these features are provided in the supplementary section.

## 2.5 Radiomic feature selection and classification

Radiomic features that were correlated with each other were discarded using Pearson's correlation coefficient at a threshold of 0.90. The best set of discriminating features between AS+ and AS- patients were identified using the maximum relevance and minimum redundancy (mRMR) feature selection method (29), which has previously shown to be useful in identifying the optimal set of radiomic features for PCa risk stratification. A random forest (RF) machine learning classifier was used to train radiomic features in conjunction with mRMR feature selection to predict biopsy upgrade in AS patients. Clinical variables including PSA, tumor volume, and age were collected from electronic health records, and their association with biopsy upgrade was evaluated. Wilcoxon rank-sum test was employed to determine statistically significant ( $p < 0.05$ ) features between AS+ and AS- cohorts. Different machine learning classifiers were constructed using radiomic features—(a) baseline radiomics ( $C_{br}$ ), (b) delta radiomics ( $C_{\Delta r}$ ), (c) integrated baseline radiomics and clinical variables ( $C_{brbcl}$ ), (d) integrated delta radiomics and baseline clinical ( $C_{\Delta r bcl}$ ), and (e) integrated delta radiomics and delta clinical ( $C_{\Delta r \Delta cl}$ ). We also compared the performance of our best machine learning classifier with a radiologist-assigned PIRADS v2.1 score at baseline and follow-up. A schematic diagram illustrating the methodology is shown in Figure 2.

## 2.6 Statistical analysis

Each classification model ( $C_{br}$ ,  $C_{bcb}$ ,  $C_{\Delta r}$ ,  $C_{\Delta r bcl}$ ,  $C_{\Delta r bcb}$  and  $C_{\Delta r \Delta cl}$ ) was trained using 100 runs of threefold cross-validation. Because of the small sample size, we did not employ an independent hold out set in our study. The classification performance was evaluated in terms of area under the receiver operating characteristics curve (AUC), sensitivity, specificity, positive predictive value (PPV), and negative predictive value (NPV). The performance of developed models was also compared with clinical attributes (PSA, tumor volume, and age) and radiologists' assessment (PIRADS v2.1) using univariate and multivariate logistic regression. Computational analysis was performed in MATLAB v2021b (Nattick, MA, USA) and R v4.1.3.

## 3 Results

Based on the inclusion criteria,  $N = 121$  PCa patients were identified with mpMRI scans available at baseline and follow-up. Of these,  $N = 17$  patients were excluded due to either poor-quality MRI, non-availability of scans, or upgraded within 1 year after baseline. Among the remaining ones, radiologists did not find any visible lesion in  $N = 48$  patient studies and were excluded. Another  $N = 6$  were discarded due to poor image quality following PIRADS v2.1 guidelines. Of the  $N = 50$  selected patients,  $N = 28$  experienced biopsy upgrade (AS+) while others retained biopsy GGG (AS-). Of these,  $N = 30$  patients had a follow-up MRI of adequate quality available, of which  $N = 19$  experienced pathologic upgrading (AS+).

### 3.1 Radiomics from baseline prostate MRI for predicting AS+

In this experiment, we aimed to evaluate radiomics of PCa lesions at baseline bpMRI in predicting pathologic upgrade in AS patients (AS+). Radiomic features at baseline ( $F_{br}$ ) including Haralick (sum of entropy, sum of variance, and difference entropy) features from T2W and Haralick and CoLIAGe energy

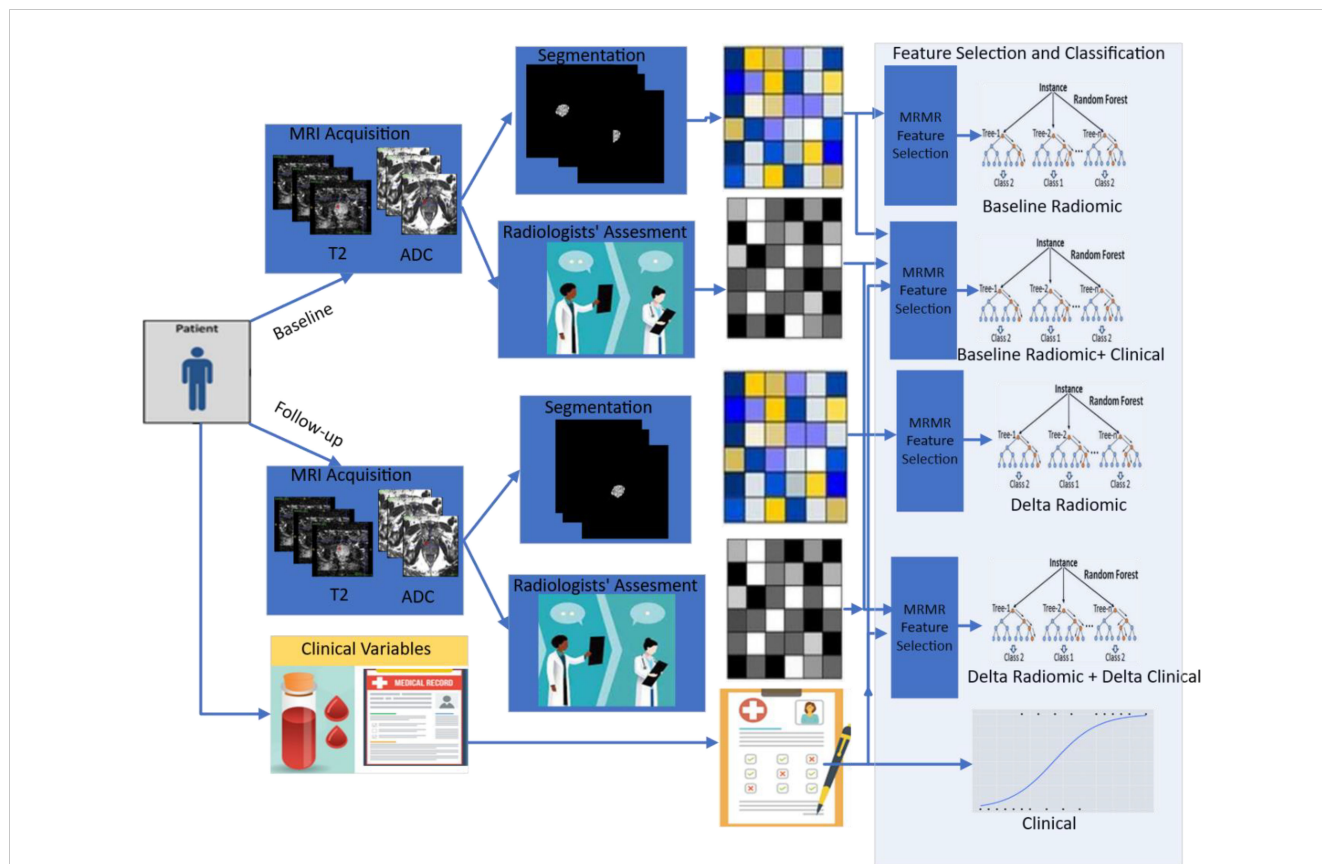


**FIGURE 2**  
 Pipeline used in this study illustrating radiomics from serial prostate biparametric MRI to predict pathologic progression in prostate cancer patients on AS. Radiomic features are extracted from prostate cancer regions of interest delineated by experienced radiologists at baseline and follow-up, which are then integrated with clinical variables in different combinations to build machine learning models (baseline radiomics, baseline radiomics + clinical, delta radiomics, delta radiomics + delta clinical, and clinical).

features from ADC maps were significantly associated with AS+ ( $p < 0.05$ ) (Table 4). We observed that gray-level and gradient-level co-occurrence (quantified by Haralick and CoLIAGe features) from baseline bpMRI (T2W and ADC) were associated with pathologic progression on AS as illustrated in terms of radiomic feature maps in Figure 3. These features essentially capture intensity and gradient-based heterogeneity through statistics of corresponding co-occurrence matrices. Radiomic classifier ( $C_{br}$ ) trained using baseline radiomics ( $F_{br}$ ) from ADC and T2W resulted in AUC =  $0.56 \pm 0.05$  and  $0.58 \pm 0.06$ , respectively. Combined radiomic features from T2W and ADC resulted in improved classification performance AUC =  $0.64 \pm 0.09$ . The improvement is statistically significant ( $p < 0.05$ ).

### 3.2 Delta radiomics from prostate MRI for prediction of AS+

In this experiment, we evaluated the association between delta radiomics  $F_{\Delta r}$  (computed as the difference in radiomics of PCA lesion between baseline and follow-up MRI) and pathologic upgrading on biopsy. Delta radiomics  $F_{\Delta r}$  including Haralick features (difference of entropy and sum of variance) from T2W and Haralick features (entropy, energy, and diagonal difference)

from ADC were observed to be associated with AS+. Machine learning classifier ( $C_{\Delta r}$ ) trained using delta radiomic features from T2W and ADC resulted in AUCs of  $0.71 \pm 0.08$  and  $0.72 \pm 0.12$ , respectively. Combining T2W and ADC delta radiomics resulted in an AUC =  $0.74 \pm 0.15$ . The classification performance metrics are provided in Table 5.

### 3.3 Integrated nomogram with clinical variables, baseline, and delta radiomics

We integrated clinical parameters including PSA, tumor volume, and age with the risk scores estimated from classifiers ( $C_{br}$ ,  $C_{\Delta r}$ , and  $C_{bcl}$ ) to develop integrated classifiers  $C_{\Delta r b c b}$ ,  $C_{\Delta r b c b}$  and  $C_{\Delta r \Delta c l}$  for predicting AS+. Clinical parameters including PSA, tumor volume, age at diagnosis, and PIRADS v2.1 at baseline were evaluated for their association with AS+. On univariate analysis, PIRADS v2.1, PSA, and tumor volume were found to be significantly associated ( $p < 0.05$ ) with AS+, resulting in AUCs of  $0.62 \pm 0.1$ ,  $0.61 \pm 0.08$ , and  $0.67 \pm 0.12$ , respectively. An integrated model ( $C_{br b c l}$ ) combining baseline radiomics and significant baseline clinical parameters (PSA and tumor volume) delivered an AUC of  $0.70 \pm 0.18$ . In comparison, PIRADS v2.1 scores from baseline resulted in an AUC =  $0.62 \pm 0.05$ , indicating that our

TABLE 4 Top three frequently selected features with their *p*-value.

Experiment	Imaging type	Feature name	p-value
$C_{br}$	T2W	Kurtosis of Haralick's sum of entropy	0.0067
		Kurtosis of Haralick's sum of variance	0.0158
		Mean of Haralick's difference entropy	0.0028
	ADC	Skewness of Haralick's energy	0.1755
		Mean of CoLiAGe	0.0325
		Variance of Haralick's energy	0.0325
$C_{\Delta r}$	T2W	Mean of Haralick's difference entropy	0.0032
		Kurtosis of Haralick's sum of variance	0.0062
		Skewness of Haralick's difference entropy	0.0007
	ADC	Mean of Haralick's entropy	0.0050
		Kurtosis of Haralick's energy	0.0617
		Kurtosis of diagonal difference	0.0302

integrated model  $C_{brbcl}$  significantly outperformed PIRADS v2.1 scores.

We integrated significant clinical variables (PSA and tumor volume) at baseline with  $F_{\Delta r}$  to build an integrated model ( $C_{\Delta r bcl}$ ) that resulted in an AUC of  $0.77 \pm 0.23$ . Finally, we developed

another integrated model ( $C_{\Delta r \Delta cl}$ ) combining delta radiomics and delta clinical variables (PSA and tumor volume) delivering the highest AUC of  $0.84 \pm 0.20$ .  $C_{\Delta r \Delta cl}$  also significantly outperformed PIRADS v2.1 scores at baseline and follow-up in predicting AS+ (AUC = 0.62 and 0.67, respectively, for baseline and follow-up).

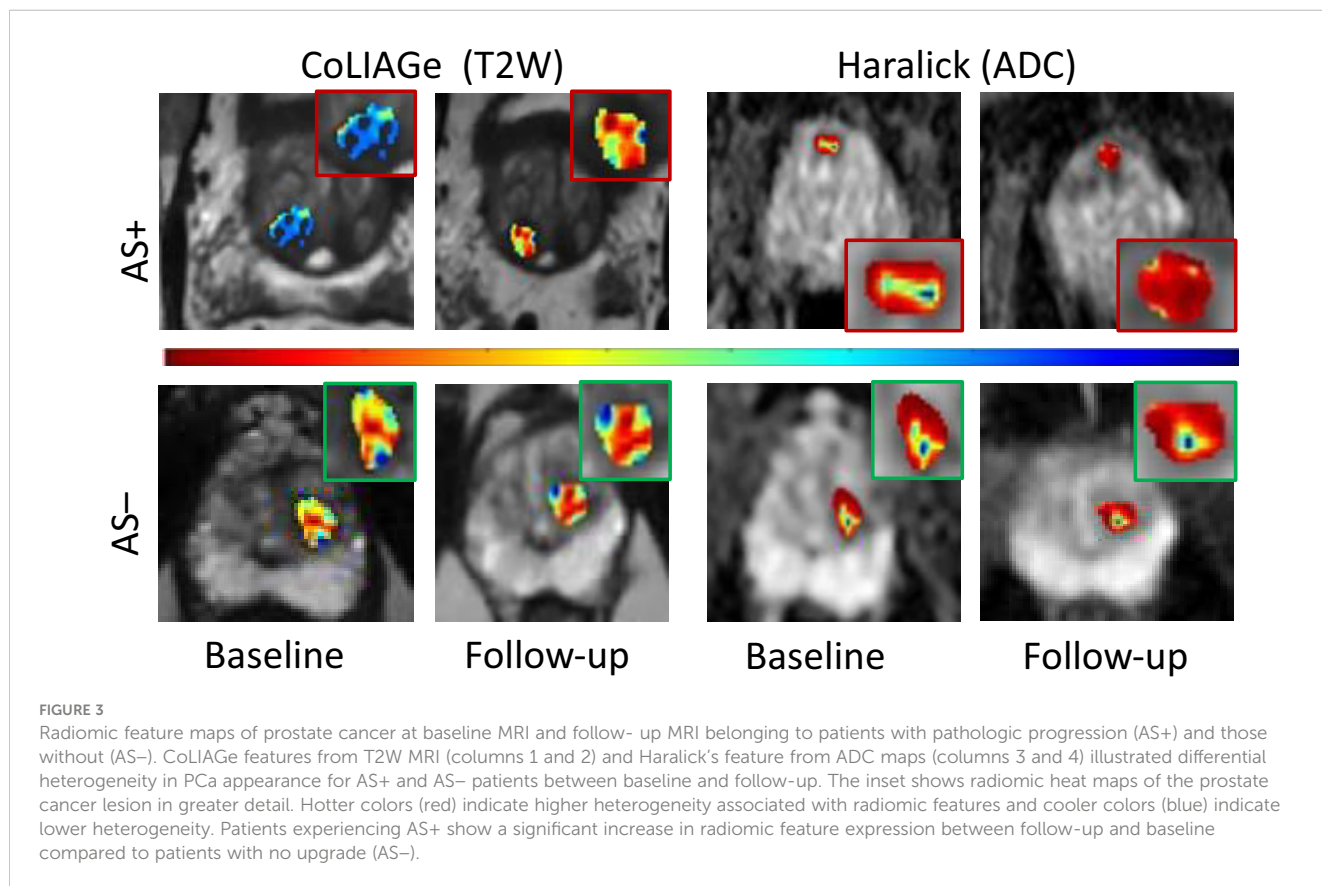


TABLE 5 Performance evaluation of predictive power of imaging, clinical model from baseline, as well delta radiomics in terms of accuracy, sensitivity, specificity, PPV (positive predictive value), NPV (negative predictive value) maximizing sensitivity, and specificity.

	Experiments	Accuracy	Sensitivity	Specificity	PPV	NPV
<b>Baseline</b> (n = 50)	T2W	0.50 ± 0.09	0.65 ± 0.21	0.41 ± 0.13	0.43 ± 0.05	0.71 ± 0.06
	ADC	0.56 ± 0.10	0.66 ± 0.22	0.50 ± 0.29	0.50 ± 0.15	0.77 ± 0.11
	T2W + ADC ( $C_{br}$ )	0.57 ± 0.10	0.61 ± 0.27	0.53 ± 0.28	0.50 ± 0.14	0.73 ± 0.11
	PSA	0.50 ± .010	0.67 ± 0.31	0.40 ± 0.33	0.42 ± 0.06	0.75 ± 0.13
	PIRADS	0.71 ± .004	0.37 ± 0.08	0.91 ± 0.09	0.75 ± 0.13	0.71 ± .002
	Tumor volume	0.79 ± 0.03	0.69 ± 0.04	0.89 ± 0.05	0.84 ± 0.05	0.77 ± 0.02
	Imaging + Cl ( $C_{brbcl}$ )	0.59 ± 0.08	0.71 ± 0.21	0.51 ± 0.24	0.49 ± 0.11	0.80 ± 0.11
<b>Delta Radiomics</b> (n = 30)	T2W	0.72 ± 0.07	0.81 ± 0.19	0.67 ± 0.16	0.62 ± 0.11	0.88 ± 0.09
	ADC	0.73 ± .07	0.82 ± 0.15	0.68 ± 0.15	0.62 ± 0.09	<b>0.89 ± 0.07</b>
	T2W + ADC ( $C_{\Delta r}$ )	0.75 ± 0.06	0.78 ± 0.17	0.73 ± 0.13	0.65 ± 0.11	0.87 ± 0.088
	Change in PIRADS	0.50 ± 0.05	0.67 ± 0.04	0.45 ± 0.03	0.58 ± 0.02	0.58 ± 0.01
	Imaging + Cl at baseline ( $C_{\Delta r bcl}$ )	0.67 ± 0.08	0.76 ± 0.15	0.60 ± 0.20	0.64 ± 0.10	0.78 ± 0.11
	Imaging+ delta Cl ( $C_{\Delta r \Delta cl}$ )	<b>0.81 ± 0.05</b>	<b>0.83 ± 0.13</b>	<b>0.78 ± 0.16</b>	<b>0.77 ± 0.13</b>	0.87 ± 0.08

$C_{br}$  = Baseline radiomics model,  $C_{brbcl}$  = Baseline radiomics + baseline clinical model,  $C_{\Delta r}$  = Delta radiomics model,  $C_{\Delta r bcl}$  = Delta radiomics + baseline clinical,  $C_{\Delta r \Delta cl}$  = Delta radiomics + delta clinical model. The bold face denotes the best performance for each performance evaluation index.

ROC curves resulting from  $C_{br}$ ,  $C_{\Delta r}$ ,  $C_{brbcl}$ ,  $C_{\Delta r bcl}$  and  $C_{\Delta r \Delta cl}$  are illustrated in Figure 4. Detailed results corresponding to these classifiers are provided in Table 5. The improvement obtained by combining delta radiomics and delta clinical was statistically significant over other combinations. Additionally, specificity, PPV, and NPV metrics computed at 90% sensitivity are provided in Table 6.

### 4 Discussion

The current standard of care for identifying and monitoring PCa patients on AS involves PSA tests, invasive biopsies, and DRE (3–5). While serial MRI is being widely incorporated into the AS setting, several long-term studies (10, 30) have indicated that serial MRI alone cannot be reliably used to monitor progression. This is

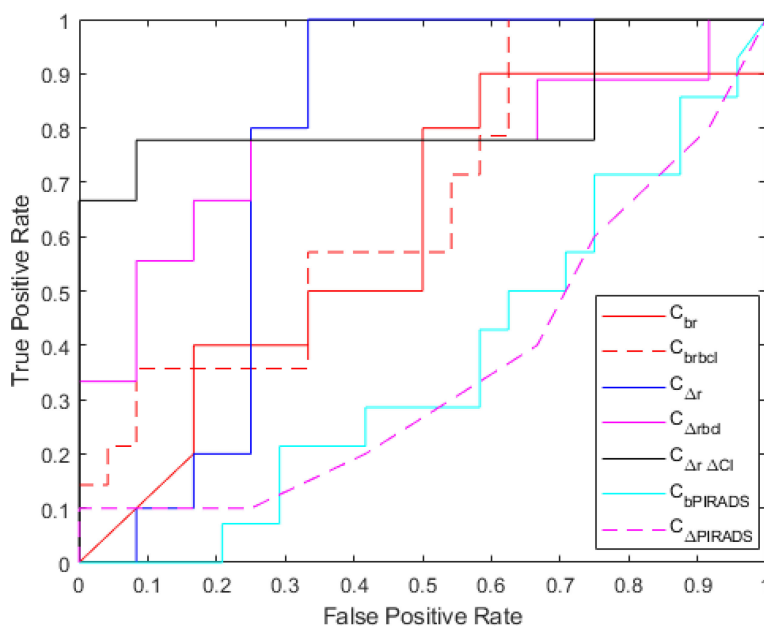


FIGURE 4 Receiver operating characteristics curve for baseline radiomics ( $C_{br}$ ), baseline radiomics + baseline clinical ( $C_{brbcl}$ ), delta radiomics ( $C_{\Delta r}$ ), delta radiomics + baseline clinical ( $C_{\Delta r bcl}$ ), delta radiomics + delta clinical ( $C_{\Delta r \Delta cl}$ ), baseline PIRADS ( $C_{bPIRADS}$ ), and delta PIRADS ( $C_{\Delta PIRADS}$ ).



TABLE 6 Specificity, PPV, and NPV of different predictive models at 90% sensitivity.

	Experiments	Specificity	PPV	NPV
<b>Baseline</b> ( <i>n</i> = 50)	T2W	0.21	0.39	0.71
	ADC	0.38	0.44	0.82
	T2W + ADC ( $C_{br}$ )	0.41	0.53	0.83
	PSA	0.08	0.35	0.50
	PIRADS	0.17	0.33	0.50
	Tumor volume	0.08	0.35	0.50
	Imaging + Cl ( $C_{brbcl}$ )	0.17	0.39	0.80
<b>Delta Radiomics</b> ( <i>n</i> = 30)	T2W	0.17	0.44	0.67
	ADC	0.08	0.42	0.50
	T2W + ADC ( $C_{\Delta r}$ )	0.25	0.47	0.75
	Imaging + Cl at baseline ( $C_{\Delta r bcl}$ )	0.42	0.53	0.83
	Imaging + delta Cl ( $C_{\Delta r \Delta cl}$ )	0.75	0.73	0.90

due to its low positive predictive value and presence of invisible and benign confounding tumor appearances (10, 30). In this preliminary proof-of-concept study, we explored the role of radiomics from baseline and follow-up serial bi-parametric prostate MRI in conjunction with clinical parameters in order to evaluate association with pathologic progression on biopsy. A biopsy upgrade (AS+) was defined as an increase in GGG from baseline 1 to  $\geq 2$  (increase in number of positive cores for baseline GGG = 2) at follow-up and no upgrade (AS-) when GGG remained the same. To the best of our knowledge, our study is one of the first attempts at exploring the combination of change in routinely acquired clinical parameters with handcrafted radiomics from serial MRI to predict pathologic progression in AS patients. We observed that radiologic progression of PCa captured by delta radiomic features (specifically Haralick and CoLLAGE features) between baseline and follow-up MRI was significantly associated with pathologic progression on biopsy (AS+). These features essentially capture intensity and gradient-based heterogeneity through statistics of corresponding co-occurrence matrices. A machine learning classifier trained using delta radiomic features showed stronger association with biopsy upgrade compared to baseline radiomics (AUC = 0.74 vs. 0.71) and radiologist-assigned PIRADS v2.1 scores (AUC = 0.62). Integrating delta radiomics with changes in clinical parameters (PSA and tumor volume) between baseline and follow-up resulted in the best classification model in predicting AS+ (AUC = 0.81).

Baseline bp-MRI has been shown to be promising in predicting pathologic upgrading in patients on AS (14). Studies (31, 32) have shown that PIRADS  $\geq 3$  have a positive predictive value of 35%–40% for reclassification at 3 years. While this is insufficient to recommend the use of MRI alone for AS (10, 33), it suggests that features associated with aggressive PCa that would go on to experience biopsy progression can be observed on MRI. In addition, the presence of MRI invisible PCa lesions precludes the possibility of obviating confirmatory biopsies (32) as indicated by the MRIAS trial (32). Since patients on AS are characterized by low-

risk disease, radiomic features capable of capturing subtle, subvisual characteristics of future progression need to be identified. We observed that quantitative radiomic features related to intensity and gradient-based heterogeneity on MRI were associated with pathologic upgrading in PCa patients on AS. Interestingly, in addition to the baseline radiomics, we observed that PIRADS v2.1, PSA, and tumor volume at baseline were strongly associated with AS+ (AUC = 0.61, 0.62, and 0.67). However, sensitivity of PIRADS v2.1 was found to be poor in our study, suggesting that PIRADS v2.1 may miss detecting pathologic progression (AS+). Although PIRADS v2.1 was not developed for predicting pathologic upgrade for AS, PIRADS  $\geq 3$  at follow-up and increase in PIRADS score of a lesion between baseline and follow-up are a non-invasive estimation of clinically significant PCa at follow-up. This indicates that radiological progression may be associated with increase in biopsy GGG on AS.

A few recent studies have explored artificial intelligence (AI)-based approaches using baseline MRI for predicting biopsy upgrading in PCa patients on AS. Sushentsev et al. (31) demonstrated that radiomics from baseline bpMRI were significantly associated with pathologic progression in PCa patients. However, they noticed incremental benefit with the addition of clinical parameters. Another study by Xie et al. investigated the role of radiomics from ADC maps to predict upgrading in Gleason score from TRUS-guided biopsies to radical prostatectomy (34). While Xie et al.'s study (34) did not directly address progression on repeat biopsy, they demonstrated that radiomic features from screening MRI can differentiate clinically significant and insignificant PCa.

Serial MRI is being actively explored for monitoring tumor progression in patients on AS as opposed to protocol-based biopsies (35). However, lesion visibility and limited PIRADS v2.1 accuracy continue to limit its potential for non-invasive monitoring. In our study, we observed that radiological tumor progression quantified using delta radiomics (intensity co-occurrence features from T2W and ADC) showed significant association with pathologic

progression (Figure 3). These features reflect intensity and gradient-based subvisual heterogeneity attributes that are potentially associated with pathologic progression. We demonstrated that the delta-radiomics risk score is associated with clinical trajectory of the cancer lesion towards pathologic progression on AS and is better associated with biopsy upgrade compared to PIRADS or change in PIRADS on follow-up.

A closely related study by Sushentsev et al. also demonstrated that delta radiomics from PCa ROIs on serial bpMRI were associated with pathologic progression in patients on AS (36). They also observed that Haralick (co-occurrence) features from T2W and ADC were associated with PCa progression. However, in our study, we leveraged novel radiomic features including CoLLAGe, which aims to quantify gradient-based tissue heterogeneity; these features have been previously shown to be associated with aggressive PCa (37–39). While the Sushentsev study (36) compared delta radiomics from MRI against PRECISE score (16) for predicting pathologic progression, we integrated delta radiomics with delta changes in PSA and tumor volume; this combined model yielded the best prediction results. We also evaluated radiomic features at baseline and in combination with routine clinical parameters (PSA and tumor volume) for their association with AS+, corroborating the idea of dynamic monitoring using MRI and PSA dynamics (40). We ensured strict controls and blinded our readers to pathologic findings to minimize reader bias; it is unclear whether such precautions to mitigate potential bias were invoked in the study of Sushentsev et al. (36). AUC reported in their study (36) was comparable to our  $C_{\Delta r, \Delta t}$  model; however, their approach (36) relies on a qualitative PRECISE score that is susceptible to inter-observer variability. This is different compared to quantitative radiomic texture measurements. Moreover, our dataset is different from the dataset used in Sushentsev et al. (36); thus, it may not be possible to perform a precise comparison.

Another related study was the one by Roest et al. who developed a deep learning model using serial MRI for monitoring PCa progression (41). They built a U-Net-based deep learning model to detect clinically significant prostate cancer (csPCa) at baseline and follow-up MRI, and extract differential tumor volume and csPCa likelihood scores, which were then used to train a supervised machine learning model to detect csPCa. They trained the csPCa detection model on patients with screening MRI who were not enrolled on AS and evaluated it for identification of csPCa on AS patients with serial MRI. However, their method relies on deep learning for detection of csPCa. Despite recent works aimed at improving interpretability (42–44), deep learning essentially is a black box-based approach that may not allow for biological interpretation of signatures associated with PCa progression. Moreover, deep learning approaches were found to fail to converge and generalize in the absence of a large dataset as demonstrated in a recent study of machine learning for treatment response prediction in ophthalmology images by Dong et al. (45).

Our approach, on the other hand, involved the use of handcrafted radiomic features explicitly associated with PCa progression from radiologist-identified PCa ROIs on MRI; these

features were subsequently found to be associated with pathologic progression. Similar to our study, the findings from Roest et al. indicate that computationally derived features from serial prostate MRI can enable non-invasive surveillance. Serial MRI in conjunction with PSA kinetics is becoming increasingly popular as an alternative to unnecessary repeat biopsies (18). Results from our study also reflect the potential opportunity for dynamic monitoring using repeat MRI and PSA density trends for men with PCa on AS (35).

Our study, however, had several limitations. Firstly, the sample size of the dataset used in the development of baseline and delta radiomic models was small. A large number of patients were excluded due to the presence of MRI non-visible PCa lesions. Owing to the small sample size, we could only report cross-validation results without testing on a hold-out validation set. However, our sample size is comparable to other radiomic studies in the context of AS including those of Sushentsev et al. (31, 36) and Algohary et al. (46). Even the study by Roest et al. (41) employed a comparably sized set of patients. Additionally, our findings suggest the presence of a strong association between delta radiomics in combination with a change in clinical variables and biopsy upgrade. Our results were in agreement with those reported by other groups (31, 34). Second, pathologic progression was estimated using systematic biopsy, which may not be as accurate as MRI-targeted biopsy (47). However, we ensured that the positive biopsy core locations matched with the location of blinded ROI delineations by the radiologists. We also ensured that the same lesion at baseline was being followed up on serial MRI. Thirdly, two readers were involved in this study and inter-observer differences in PIRADS v2.1 and ROI delineations may have impacted radiomic feature extraction. However, a small subset of cases ( $N = 15$ ) were read by the two readers and a reasonably good inter-reader agreement in ROI ( $\kappa = 0.80$ ) was determined. In future work, we will also seek to quantitatively assess the impact of inter-reader variation on a larger number of cases. Fourth, the difference between baseline and follow-up MRI was not consistent across all patients since this was a retrospective cohort. Nevertheless, we limited the follow-up MRI at 3 years with a range of  $\pm 12$  months to ensure a relatively homogeneous follow-up. Lastly, radiologists missed a significant number of PCa lesions at baseline due to poor diagnostic quality or the presence of non-visible lesions given that they were blinded to biopsy results. This was made to ensure that no reader bias was introduced in obtaining PCa ROIs on MRI.

In summary, preliminary findings from our single-center study suggest that quantitative radiomic features derived from baseline and serial MRI are associated with biopsy upgrade on AS. Delta radiomics from serial MRI in conjunction with routine clinical parameters (including PSA and tumor volume) may be used to non-invasively predict pathologic progression in PCa patients on AS. Our findings align with those from previous studies (36, 41, 48), which suggest that machine learning and deep learning approaches with prostate MRI can enable non-invasive monitoring of patients on AS. Future directions will involve large-scale multisite validation of delta radiomics approaches from serial MRI, automated and

reliable pipelines for lesion detection, and prospectively validating these approaches in a clinical setting.

## Data availability statement

The raw data supporting the conclusions of this article will be made available by the authors following institutional guidelines, without undue reservation. Requests to access the data should be directed to the corresponding authors.

## Ethics statement

The studies involving human participants were reviewed and approved by University Hospitals Cleveland Medical Center, Cleveland 06-16-30C. The patients/participants provided their written informed consent to participate in this study.

## Author contributions

AbM contributed to the experimental design, analysis, software, writing. AH and JH contributed to the software, data analysis. VV helped with the data acquisition, data preprocessing, and writing. DL and AnM contributed data collection. LB and ST contributed to the imaging interpretation data preparation, and writing. acquisition, funding, and clinical interpretation. LP contributed to the data collection and conception of idea. AnM and RS contributed to the conception of the idea, experimental design, supervision, writing, and funding. All authors contributed to the article and approved the submitted version.

## Funding

Research reported in this publication was supported by the National Cancer Institute under award numbers R01CA268287A1, U01CA269181, R01CA26820701A1, R01CA249992-01A1, R01CA202752-01A1, R01CA208236-01A1, R01CA216579-01A1, R01CA220581-01A1, R01CA257612-01A1, 1U01CA239055-01, 1U01CA248226-01, 1U54CA254566-01, National Heart, Lung and Blood Institute 1R01HL15127701A1, R01HL15807101A1, National Institute of Biomedical Imaging and Bioengineering 1R43EB028736-01, VA Merit Review Award IBX004121A from the United States Department of Veterans Affairs Biomedical Laboratory Research and Development Service, the Office of the Assistant Secretary of Defense for Health Affairs, through the Breast Cancer Research Program (W81XWH-19-1-0668), the Prostate Cancer Research Program (W81XWH-20-1-0851), the Lung Cancer Research Program (W81XWH-18-1-0440 and W81XWH-20-1-0595), the Peer Reviewed Cancer Research

Program (W81XWH-18-1-0404, W81XWH-21-1-0345, and W81XWH-21-1-0160), (W81XWH-22-1-0236) the Kidney Precision Medicine Project (KPMP) Glue Grant, sponsored research agreements from Bristol Myers-Squibb, Boehringer-Ingelheim, Eli-Lilly, and AstraZeneca, American Cancer Society Institutional Research Grant from Winship Cancer Institute, and Winship Invest\$ Pilot Grant from the Winship Cancer Institute.

## Conflict of interest

Author AnM is an equity holder in the company Elucid Bioimaging and Inspirata Inc. He is also a scientific advisory consultant for Inspirata Inc. In addition, he has served as a scientific advisory board member for Inspirata Inc., AstraZeneca, Bristol Meyers-Squibb, and Merck. He also has sponsored research agreements with Philips and Inspirata Inc. His technology has been licensed to Elucid Bioimaging and Inspirata Inc. He is also involved in an NIH U24 grant with PathCore Inc. and three different R01 grants with Inspirata Inc. AH is currently working in Picture Health, Cleveland, OH. No products from these associations are used in this study.

The remaining authors declare that the research was conducted in the absence of any commercial or financial relationships that could be construed as a potential conflict of interest.

## Publisher's note

All claims expressed in this article are solely those of the authors and do not necessarily represent those of their affiliated organizations, or those of the publisher, the editors and the reviewers. Any product that may be evaluated in this article, or claim that may be made by its manufacturer, is not guaranteed or endorsed by the publisher.

## Author disclaimer

The content is solely the responsibility of the authors and does not necessarily represent the official views of the National Institutes of Health, the U.S. Department of Veterans Affairs, the Department of Defense, or the United States Government.

## Supplementary material

The Supplementary Material for this article can be found online at: <https://www.frontiersin.org/articles/10.3389/fonc.2023.1166047/full#supplementary-material>

## References

- American Cancer Society. *Cancer Facts & Figures*. Atlanta (2022). p. 2022. Available at: <https://www.cancer.org/content/dam/cancer-org/research/cancer-facts-and-statistics/annual-cancer-facts-and-figures/2022/2022-cancer-facts-and-figures.pdf>.
- Drost F-JH, Rannikko A, Valdagni R, Pickles T, Kakehi Y, Remmers S, et al. Can active surveillance really reduce the harms of overdiagnosing prostate cancer? A reflection of real life clinical practice in the PRIAS study. *Transl Androl Urol* (2018) 7:9805–105. doi: 10.21037/tau.2017.12.28
- Chen RC, Rumble RB, Loblaw DA, Finelli A, Ehdai B, Cooperberg MR, et al. Active surveillance for the management of localized prostate cancer (Cancer care Ontario guideline): American society of clinical oncology clinical practice guideline endorsement. *J Clin Oncol Off J Am Soc Clin Oncol* (2016) 34:2182–90. doi: 10.1200/JCO.2015.65.7759
- Carroll PH, Mohler JL. NCCN guidelines updates: prostate cancer and prostate cancer early detection. *J Natl Compr Cancer Netw JNCCN* (2018) 16:620–3. doi: 10.6004/jnccn.2018.0036
- National Comprehensive Cancer Network (NCCN). *Prostate Cancer Early Stage* (2020).
- Porten SP, Whitson JM, Cowan JE, Cooperberg MR, Shinohara K, Perez N, et al. Changes in prostate cancer grade on serial biopsy in men undergoing active surveillance. *J Clin Oncol Off J Am Soc Clin Oncol* (2011) 29:2795–800. doi: 10.1200/JCO.2010.33.0134
- Elkhoury FF, Felker ER, Kwan L, Sisk AE, Delfin M, Natarajan S, et al. Comparison of targeted vs systematic prostate biopsy in men who are biopsy naive: the prospective assessment of image registration in the diagnosis of prostate cancer (PAIREDCAP) study. *JAMA Surg* (2019) 154:811. doi: 10.1001/jamasurg.2019.1734
- Wade J, Donovan J, Lane A, Davis M, Walsh E, Neal D, et al. Strategies adopted by men to deal with uncertainty and anxiety when following an active surveillance/monitoring protocol for localised prostate cancer and implications for care: a longitudinal qualitative study embedded within the ProtecT trial. *BMJ Open* (2020) 10:e036024. doi: 10.1136/bmjopen-2019-036024
- Bailey DE, Wallace M, Latini DM, Hegarty J, Carroll PR, Klein EA, et al. Measuring illness uncertainty in men undergoing active surveillance for prostate cancer. *Appl Nurs Res* (2011) 24:193–9. doi: 10.1016/j.apnr.2009.08.001
- Rajwa P, Pradere B, Quhal F, Mori K, Laukhtina E, Huebner NA, et al. Reliability of serial prostate magnetic resonance imaging to detect prostate cancer progression during active surveillance: A systematic review and meta-analysis. *Eur Urol* (2021) 80:549–63. doi: 10.1016/j.eururo.2021.05.001
- Kinsella N, Helleman J, Bruinsma S, Carlsson S, Cahill D, Brown C, et al. Active surveillance for prostate cancer: a systematic review of contemporary worldwide practices. *Transl Androl Urol* (2018) 7:83–97. doi: 10.21037/tau.2017.12.24
- Naji L, Randhawa H, Sohani Z, Dennis B, Lautenbach D, Kavanagh O, et al. Digital rectal examination for prostate cancer screening in primary care: A systematic review and meta-analysis. *Ann Fam Med* (2018) 16:149–54. doi: 10.1370/afm.2205
- Osses DF, Drost FH, Verbeek JFM, Luiting HB, van Leenders GJLH, Bangma CH, et al. Prostate cancer upgrading with serial prostate magnetic resonance imaging and repeat biopsy in men on active surveillance: are confirmatory biopsies still necessary? *BJU Int* (2020) 126:124–32. doi: 10.1111/bju.15065
- Dominique G, Brisbane WG, Reiter RE. The utility of prostate MRI within active surveillance: description of the evidence. *World J Urol* (2022) 40:71–7. doi: 10.1007/s00345-021-03853-9
- Kang SK, Mali RD, Prabhu V, Ferket BS, Loeb S. Active surveillance strategies for low-grade prostate cancer: comparative benefits and cost-effectiveness. *Radiology* (2021) 300:594–604. doi: 10.1148/radiol.2021204321
- Moore CM, Giganti F, Albertsen P, Allen C, Bangma C, Briganti A, et al. Reporting magnetic resonance imaging in men on active surveillance for prostate cancer: the PRECISE recommendations—A report of a European School of oncology task force. *Eur Urol* (2017) 71:648–55. doi: 10.1016/j.eururo.2016.06.011
- Ediz C, Akan S, Temel MC, Yilmaz O. The importance of PSA-Density in active surveillance for prostate cancer. *Arch Ital Urol E Androl* (2020) 92. doi: 10.4081/aiua.2020.2.136
- Stavriniades V, Papageorgiou G, Danks D, Giganti F, Pashayan N, Trock B, et al. Mapping PSA density to outcome of MRI-based active surveillance for prostate cancer through joint longitudinal-survival models. *Prostate Cancer Prostatic Dis* (2021) 24:1028–31. doi: 10.1038/s41391-021-00373-w
- Alghohary A, Shiradkar R, Pahwa S, Purysko A, Verma S, Moses D, et al. Combination of peri-tumoral and intra-tumoral radiomic features on bi-parametric MRI accurately stratifies prostate cancer risk: A multi-site study. *Cancers* (2020) 12. doi: 10.3390/cancers12082200
- Xu L, Zhang G, Shi B, Liu Y, Zou T, Yan W, et al. Comparison of biparametric and multiparametric MRI in the diagnosis of prostate cancer. *Cancer Imaging* (2019) 19:90. doi: 10.1186/s40644-019-0274-9
- Woo S, Suh CH, Kim SY, Cho JY, Kim SH, Moon MH Head-to-head comparison between biparametric and multiparametric MRI for the diagnosis of prostate cancer: A systematic review and meta-analysis. *Am J Roentgenol* (2018) 211:W226–41. doi: 10.2214/AJR.18.19880
- MD.ai. The platform for medical AI. Available at: [www.MD.ai](http://www.MD.ai).
- Klein S, Staring M, Murphy K, Viergever MA, Pluim J. elastix: A toolbox for intensity-based medical image registration. *IEEE Trans Med Imaging* (2010) 29:196–205. doi: 10.1109/TMI.2009.2035616
- Shamonin D. Fast parallel image registration on CPU and GPU for diagnostic classification of Alzheimer's disease. *Front Neuroinformatics* (2013) 7. doi: 10.3389/fninf.2013.00050
- Nyúl LG, Udupa JK. On standardizing the MR image intensity scale. *Magn Reson Med* (1999) 42:1072–81. doi: 10.1002/(SICI)1522-2594(199912)42:6<1072::AID-MRM11>3.0.CO;2-M
- Haralick RM, Shanmugam K, Dinstein I. Textural features for image classification. *IEEE Trans Syst Man Cybern* (1973) SMC-3(6):610–21. doi: 10.1109/TSMC.1973.4309314
- Prasanna P, Tiwari P, Madabhushi A. Co-occurrence of Local Anisotropic Gradient Orientations (CoLAgE): A new radiomics descriptor. *Sci Rep* (2016) 6:37241. doi: 10.1038/srep37241
- Zwanenburg A, Vallières M, Abdalah MA, Aerts HJWL, Andrearczyk V, Apte A, et al. The image biomarker standardization initiative: standardized quantitative radiomics for high-throughput image-based phenotyping. *Radiol* (2020) 295:328–38. doi: 10.1148/radiol.2020191145
- Peng H, Long F, Ding C. Feature selection based on mutual information: criteria of max-dependency, max-relevance, and min-redundancy. *IEEE Trans Pattern Anal Mach Intell* (2005) 27:1226–38. doi: 10.1109/TPAMI.2005.159
- Felker ER, Wu J, Natarajan S, Margolis DJ, Raman SS, Huang J, et al. Serial magnetic resonance imaging in active surveillance of prostate cancer: incremental value. *J Urol* (2016) 195:1421–7. doi: 10.1016/j.juro.2015.11.055
- Sushentsev N, Rundo L, Blyuss O, Gnanaprasam VJ, Sala E, Barrett T MRI-derived radiomics model for baseline prediction of prostate cancer progression on active surveillance. *Sci Rep* (2021) 11:12917. doi: 10.1038/s41598-021-92341-6
- Amin A, Scheltema MJ, Shnier R, Blazevski A, Moses D, Cusick T, et al. The magnetic resonance imaging in active surveillance (MRIAS) trial: use of baseline multiparametric magnetic resonance imaging and saturation biopsy to reduce the frequency of surveillance prostate biopsies. *J Urol* (2020) 203:910–7. doi: 10.1097/JU.0000000000000693
- McGirt MJ, Villavicencio AT, Bulsara KR, Friedman AH. MRI-guided stereotactic biopsy in the diagnosis of glioma: comparison of biopsy and surgical resection specimen. *Surg Neurol* (2003) 59:277–281; discussion 281–282. doi: 10.1016/S0090-3019(03)00048-X
- Xie J, Li B, Min X, Zhang P, Fan C, Li Q, et al. Prediction of pathological upgrading at radical prostatectomy in prostate cancer eligible for active surveillance: A texture features and machine learning-based analysis of apparent diffusion coefficient maps. *Front Oncol* (2021) 10:604266. doi: 10.3389/fonc.2020.604266
- Giganti F, Stavriniades V, Moore CM. Magnetic resonance imaging-guided active surveillance of prostate cancer: time to say goodbye to protocol-based biopsies. *Eur Urol Open Sci* (2022) 38:40–3. doi: 10.1016/j.euro.2021.08.016
- Sushentsev N, Rundo L, Blyuss O, Nazarenko T, Suvorov A, Gnanaprasam VJ, et al. Comparative performance of MRI-derived PRECISE scores and delta-radiomics models for the prediction of prostate cancer progression in patients on active surveillance. *Eur Radiol* (2022) 32:680–9. doi: 10.1007/s00330-021-08151-x
- Shiradkar R, Ghose S, Jambor I, Taimen P, Ettala O, Purysko AS, et al. Radiomic features from pretreatment biparametric MRI predict prostate cancer biochemical recurrence: Preliminary findings. *J Magn Reson Imaging JMIR* (2018) 48:1626–36. doi: 10.1002/jmri.26178
- Li L, Shiradkar R, Leo P, Alghohary A, Fu P, Tirumani SH, et al. A novel imaging based Nomogram for predicting post-surgical biochemical recurrence and adverse pathology of prostate cancer from pre-operative bi-parametric MRI. *EBioMedicine* (2020) 63:103163. doi: 10.1016/j.ebiom.2020.103163
- Shiradkar R, Ghose S, Mahran A, Tirumani SH, Ponsky L, Purysko AS, et al. Prostate surface distension and tumor texture descriptors from pretreatment MRI are associated with biochemical recurrence following radical prostatectomy: Preliminary Findings. *Front Oncol* (2022) 12:841801. doi: 10.3389/fonc.2022.841801
- Gallagher KM, Christopher E, Cameron AJ, Little S, Innes A, Davis G, et al. Four-year outcomes from a multiparametric magnetic resonance imaging (MRI)-based active surveillance programme: PSA dynamics and serial MRI scans allow omission of protocol biopsies. *BJU Int* (2019) 123:429–38. doi: 10.1111/bju.14513
- Roest C, Kwee TC, Saha A, Fütterer JJ, Yakar D, Huisman H AI-assisted biparametric MRI surveillance of prostate cancer: feasibility study. *Eur Radiol* (2022) 33:89–96. doi: 10.1007/s00330-022-09032-7
- Bhatt S, Cohon A, Rose J, Majerczyk N, Cozzi B, Crenshaw D, et al. Interpretable machine learning models for clinical decision-making in a high-need, value-based primary care setting. *NEJM Catal* (2021) 2:CAT.21.0008. doi: 10.1056/CAT.21.0008
- Chakraborty S, Tomsett R, Raghavendra R, Harborne D, Alzantot M, Cerutti F, et al. (2017). Interpretability of deep learning models: A survey of results, in: *2017 IEEE SmartWorld, Ubiquitous Intelligence Computing, Advanced Trusted Computed, Scalable Computing Communications, Cloud Big Data Computing, Internet of People and Smart City Innovation (SmartWorld/SCALCOM/UIC/ATC/CBDCom/IOP/SCI)* San Francisco, CA, USA. p. 1–6. doi: 10.1109/UIC-ATC.2017.8397411

44. Zhang Y, Tino P, Leonardis A, Tang KA. Survey on neural network interpretability. *IEEE Trans Emerg Top Comput Intell* (2021) 5:726–42. doi: 10.1109/TETCI.2021.3100641
45. Dong V, Sevgi DD, Kar SS, Srivastava SK, Ehlers JP, Madabhushi A. Evaluating the utility of deep learning for predicting therapeutic response in diabetic eye disease. *Front Ophthalmol* (2022) 2:852107. doi: 10.3389/fopht.2022.852107
46. Algohary A, Viswanath S, Shiradkar R, Ghose S, Pahwa S, Moses D, et al. Radiomic features on MRI enable risk categorization of prostate cancer patients on active surveillance: Preliminary findings. *J Magn Reson Imaging JMRI* (2018) 22. doi: 10.1002/jmri.25983
47. Ahdoot M, Wilbur AR, Reese SE, Lebastchi AH, Mehralivand S, Gomella PT, et al. MRI-targeted, systematic, and combined biopsy for prostate cancer diagnosis. *N Engl J Med* (2020) 382:917–28. doi: 10.1056/NEJMoa1910038
48. Shiradkar R, Mahran A, Zuo R, Li L, Ponsky L, Tirumani SH, et al. Delta Radiomic Features from serial bi-parametric MRI are associated with biopsy upgrading of prostate cancer patients on Active Surveillance. *Proc ISMRM* (2020).